Construction and Building Materials 147 (2017) 776–789

Contents lists available at ScienceDirect

Construction and Building Materials

journal homepage: www.elsevier.com/locate/conbuildmat

Study on the optimum rice husk ash content added in asphalt binder and its modification with bio-oil

Zhenqiang Han [a,b,*], Aimin Sha [a,b], Zheng Tong [a], Zhuangzhuang Liu [a,b], Jie Gao [a,b], Xiaolong Zou [a,b], Dongdong Yuan [a]

[a] School of Highway, Chang'an University, Xi'an 710064, China
[b] Key Laboratory for Special Area Highway Engineering of Ministry of Education, Chang'an Univ., Xi'an, Shaanxi 710064, China

HIGHLIGHTS

- Rice husk ash was used as modifier to improve high temperature properties of asphalt.
- 1% and 7% were confirmed as the optimum content and upper limit for rice husk ash.
- Bio-oil improved the low temperature and fatigue property of RHA modified asphalt.
- 1% rice husk ash/20% bio-oil exhibited optimal asphalt modification effect.
- The ideal bonding system was established by cooperation of rice husk ash and bio-oil.

GRAPHICAL ABSTRACT

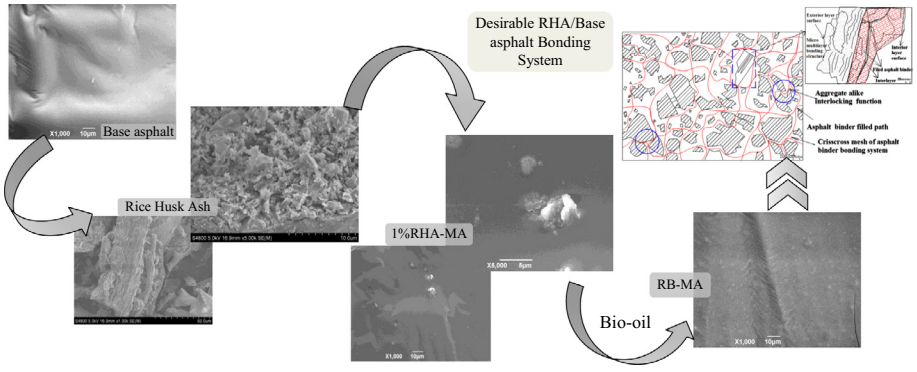

ARTICLE INFO

Article history:
Received 15 November 2016
Received in revised form 22 April 2017
Accepted 1 May 2017
Available online 8 May 2017

Keywords:
Modified asphalt
Agricultural by-products
Flexible pavement
Performance

ABSTRACT

By-products and waste materials have become the main cause of environment contamination. In this study, Rice Husk Ash (RHA) was used as modifier to improve the high temperature property of asphalt binder. Bio-oil (BO) was selected as viscosity reducer to enhance the low-temperature and anti-fatigue properties of RHA Modified Asphalt (RHA-MA). Physical and rheological indexes were measured to determine the optimal RHA and BO content. The Scanning Electron Micrographs (SEM) and Energy Dispersive Spectrometer (EDS) analysis were adopted to reveal the modification mechanism of RHA and BO. Results show that RHA-MA possessed desirable high-temperature but unsatisfactory low-temperature performance compared with base asphalt and Limestone Filler Mixed Asphalt (LA). However, asphalt binder with 1% RHA and 20% BO (RB-MA) obtained ductility (15 °C) nearly 50% higher and loss modulus approximately 20% lower than those of RHA-MA. Meanwhile, the softening point is 4.2 °C more and $G^*/\sin\delta$ at all temperatures is higher than those of BO Modified Asphalt (BA). Furthermore, SEM observation illustrates that BO is able to reduce RHA agglomeration and increase the uniformity of RHA-MA mix system, contributing greatly to the excellent comprehensive performance of RB-MA. Consequently, the joint modification of base asphalt with RHA and BO could obtain desirable high temperature, low temperature and anti-fatigue performance. Therefore, it is likely that the development of RB-MA could be helpful to make conventional asphalt qualified for complex service ambient, as well as improve the recycling rate of agricultural waste to reduce environmental pollution and reduce the life cycle cost of asphalt pavement.

* Corresponding author at: School of Highway, Chang'an University, Xi'an 710064, China.
E-mail address: jasonhan029@126.com (Z. Han).

http://dx.doi.org/10.1016/j.conbuildmat.2017.05.004
0950-0618/

1. Introduction

Rice is a fundamental source of food consumption. Due to the large demand of rice in the world market, as detailed in Table 1 [1], hundreds million tons of rice paddy are consumed yearly [2] and large quantity of rice husks are produced without proper recycling. The most prevalent way in developing countries in East and Southeast Asia is to burn rice husks directly in the filed or dump them into rivers during the farming process, causing great environmental contamination [3].

In recent years, researchers made great efforts into the utilization of RHA as supplementary building materials to decrease the pollution effect and overall construction cost. For example, RHA was used as a stabilizing agent for unstable soil treatment [4–7], as well as a supplementary cementing material for local (Egypt) construction industry [8]. As Wei [9] reported, the durability of sisal fiber reinforced cement could be enhanced by incorporating with RHA. The pozzolanic activities of RHA containing highly reactive silica was confirmed in lime-RHA or Portland-RHA cements [10] and fresh/ hardened high-performance concretes [11]. Meanwhile, the water cement ratio and RHA particle size range were also believed to affect the engineering performance of RHA-OPC system [12,13]. Furthermore, large amount of studies focused on the engineering performance comparison of cement-based composites incorporated with fly ash, silica fume and RHA, such as the shrinkage [14], compressive strength [15], self-compatibility [15], porosity and corrosion resistance [16], as well as the controlled low strength [17]. Nevertheless, it is reported that there should be a limitation of 30% (RHA replacement ratio) in the RHA-cement system [18].

To date, the functions and mechanism of RHA in Portland cement system have been well studied. Research about application in asphalt binder and asphalt concrete, however, is relatively limited. In Hot Mixed Asphalt Concrete (HMA), 50% RHA together with 50% lime stone filler were reported to efficiently improve the Marshall stability of asphalt concrete [19]. In order to study the working mechanism of RHA in asphalt binder, silane coupling agent modified nano-silica and RHA modified asphalt were investigated from the view of comprehensive performance and interface micro-structure between aggregate and asphalt, illustrating that the RHA modification effect was undesirable [20]. Besides, no chemical reactions were found between the biomass ashes (RHA and wood sawdust ash) and asphalt, and the low temperature properties of biomass ash modified asphalt was not satisfactory [21]. Apparently, previous studies are mainly focused on the high temperature and aging properties of RHA modified asphalt. However, the complicated asphalt pavement service condition demands both excellent high temperature and low temperature performance of asphalt used in the mixture. Therefore, this study aims at seeking a proper viscosity reducer compatible with RHA-MA to improve low temperature and anti-cracking properties, as well as maintain high temperature performance qualified for pavement service.

Researchers used bio-oil as alternative source of asphalt and investigated the performance of bio-binder in recent years to face the crisis of the increasingly exhausted asphalt resources. It has been reported that the bio-oil (produced from waste wood) could slightly enhance the tensile strength of asphalt mixture [22], significantly improve the low temperature anti-cracking properties [23,24]. Performance comparison of four different bio-oils (produced from Corn Stover, Miscanthus Pellet, Swine Manure and Wood Pellet) modified asphalt indicated that Wood Pellet modified asphalt had the most desirable low-temperature and rheological properties, but undesirable aging susceptibility [25]. In conclusion, bio-oils could remarkably reduce viscosity and enhance low temperature performance of asphalt binder. It seems feasible to use RHA and bio-oil as composite modifier to combine the outstanding high temperature property of RHA-MA and the excellent low temperature property of BA to obtain modified asphalt with excellent comprehensive performance.

The physical properties test (penetration, softening point and ductility test), rotational viscosity test and Dynamic Shear Rheometer (DSR) were utilized to characterize the modification effect and determine the optimal RHA and bio-oil content. Scanning Electronic Microscopy (SEM) and Energy Dispersive Spectrometer (EDS) were utilized to analyze the modification mechanism of RHA and bio-oil. The application of RHA and bio-oil is supposed to provide an environmental friendly way to prepare modified asphalt with excellent comprehensive performance with less petroleum resource consumption and lower engineering cost, as well as reduce the environment contamination caused by agricultural by-products and waste materials.

Table 1
World Rice Trade. January/December Year, Thousand Metric Tons [2].

TY exports	2012/13	2013/14	2014/15	2015/16	2016/17 Jun	2016/17 Jul
Argentina	526	494	310	480	600	600
Australia	460	404	323	180	230	200
Brazil	830	852	895	700	800	800
Burma	1163	1688	1735	1650	1750	1750
Cambodia	1075	1000	1150	900	1050	1050
China	447	393	262	350	300	300
Egypt	700	600	250	200	250	200
European Union	203	284	251	270	260	260
Guyana	346	502	536	540	540	540
India	10,480	11,588	11,046	9000	8500	8500
Pakistan	4126	3700	4000	4500	4250	4250
Paraguay	365	380	371	480	470	470
Thailand	6722	10,969	9779	9800	9000	9000
Uruguay	939	957	718	850	840	840
Vietnam	6700	6325	6606	6900	7000	7000
Others	1116	1081	1095	1091	1117	1100
Subtotal	36,198	41,217	39,327	37,891	36,957	36,860
United States	3295	2998	3472	3450	3600	3650
World Total	39,493	44,215	42,799	41,341	40,557	40,510

TY = Trade Year. Note about dates: 2015/16 is calendar year 2016, 2014/15 is calendar year 2015, and so on.

Table 2
Physical properties of base asphalt.

Penetration (25 °C, 0.1 mm)	Softening point (°C)	Ductility (15 °C,cm)	Rotational viscosity (Pa·s)	
			60 °C	135 °C
69.5	48.9	>100	191	2.724

2. Materials and methods

2.1. Materials

'Dong Hai' base asphalt (70#, JTG F40-2004 [26], Table 2) acquired from China Petrochemical industry was used. Rice husk utilized to prepare RHA was obtained from a mill in Hubei province in southern China. Properties of RHA and Limestone Filler (LF) passing through the 0.075 mm sieve are demonstrated in Table 3. Gradation of RHA and LF is presented in Fig. 1.

Bio-oil acquired from waste wood pellet was produced by a biomass energy processing plant in Shaanxi province China. Properties are shown in Table 4.

2.2. Sample preparation and tests

2.2.1. Rice husk ash preparation

RHA was obtained from controlled combustion of rich husk in a muffle. Enough air should be supplied and the burning temperature should be in the range of 500 °C and 700 °C during the 2-h combustion process, avoiding the carbonization of rice husks [3]. Afterwards, the burnt rice husk ash was milled in a ball mill for 30 min, and the used RHA was obtained by sieving the milled ash through the 0.075 mm aperture-sized sieve.

2.2.2. Modified asphalt samples preparation

RHA-MA samples with RHA (1, 3, 5, 7, 9 and 11% by mass of base asphalt) were prepared to determine the optimal RHA content. Due to the high specific surface of RHA, pre-mixing of the heated RHA and asphalt binder is necessary for easier mixing. Firstly, base asphalt and prepared RHA was heated to 150 °C in an oven and preserved for 2 h. After pre-mixing, a high-speed mixer was adopted to make the RHA mixed more uniformly with base asphalt by remaining low mix speed of 1000 r/min for 5 min and a higher speed of 3000 r/min for 15 min afterwards.

Voids and unevenness on the surface of modified asphalt can be observed after the mixing, indicating that RHA is not well dispersed. Therefore, RHA-MA was heated to 150 °C and mixed by the high-speed mixer again after 24 h. The surface of modified asphalt presented as mirror after the second mixing process, which was conceived as evidence of uniformly mixing.

The control samples (LA) with 1, 5 and 9% LF were prepared according to the same process as RHA-MA. Bio-oil Modified Asphalt (BA) samples with 15, 20, 30 and 40% bio-oil were prepared to determine the optimal bio-oil content to improve low temperature properties of modified asphalt. Similar to the modification method of RHA-MA, base asphalt was heated in the oven and preserved for 2 h. It was noteworthy that the heating temperature was set as 100 °C, taking into account that the bio-oil contains water and possesses a boiling point of 76 °C. Soon after the base asphalt was taken out of the oven, bio-oil was slowly added into the heated base asphalt with a clean glass rod stirring around, avoiding spilling caused by the boiling of bio-oil and vaporizing of water. The high-speed mixer was used to uniformly mix the BA till there are no bubbles by keeping low stirring speed of 1000 r/min for 5 min firstly and high speed of 3000 r/min for 15 min afterwards.

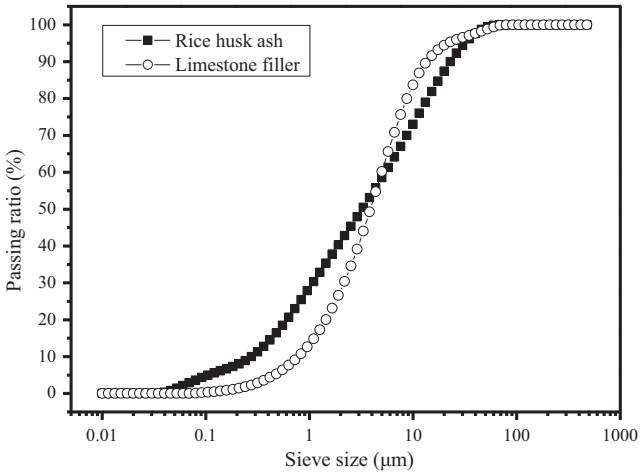

Fig. 1. Laser particle sizes test results of rice husk ash and limestone filler.

The RHA/bio-oil modified asphalt samples with optimal content of bio-oil 1, 5 and 9% content of RHA were prepared to verify the benefits that bio-oil offered to RHA-MA. Firstly, RHA was mixed with heated asphalt according to the preparation method of RHA-MA. Soon after RHA was mixed into base asphalt, the bio-oil was added into and mixed with the mixture based on the preparation procedures of BA.

The preparation methods of RHA-MA, BA and RB-MA are presented in Fig. 2. The asphalt binder samples used in this study are demonstrated in Table 5.

2.3. Physical and chemical property test of mineral filler, RHA and bio-oil

The micro-structure of RHA was observed via Hitachi S-4800 Scanning Electronic Microscopy (SEM) at the acceleration voltage of 5 kV.

Malvern laser particle sizes analyzer (MS 2000) and BET N_2 absorption apparatus (ST-2000) were adopted to characterize the particle gradation and specific surface area of RHA and LF (see Fig. 1). Clean water was used as the dispersant in the particle size

Table 3
Physical and chemical properties of rice husk ash and limestone filler.

	Physical properties				Chemical properties			
	Specific surface (cm^2/g)	Specific gravity (g/cm^2)	Bulk density (g/cm^3)	Silicon dioxide (SiO_2/%)	Calcium oxide (CaO/%)	Potassium oxide (K_2O/%)	Aluminum oxide (Al_2O_3/%)	Others (%)
RHA	4450	2.53	–	88.84	1.60	3.99	0.55	5.02
Limestone filler	3440	–	2.6	–	–	–	–	–

Table 4
Chemical and physical properties of bio-oil.

Biomass oil indexes	Chemical composite percentage w (%)				Density (g/cm^3)	pH
	w_C	w_H	w_O	w_N		
Test results	53–55	7.5–9.2	34–46	0–0.5	1.15	2.7

Note: WC, WH, WO, WN: mass percentage of carbon, hydrogen, oxygen and nitrogen element in biomass oil utilized in this study, respectively.

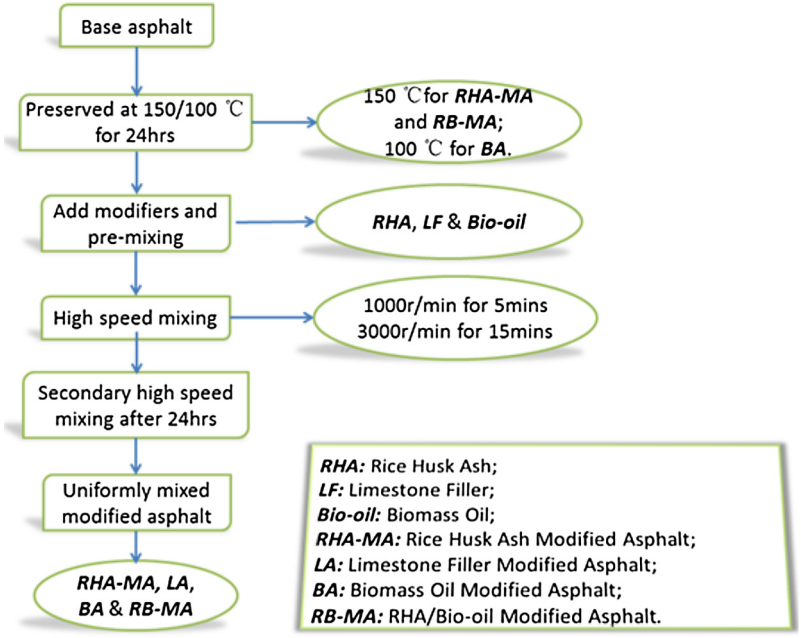

Fig. 2. Preparation methods of modified asphalt.

Table 5
Description of different modified asphalt binders used in this study.

Binder no.	Binder identification	Asphalt binders component	Component proportion (by mass)
1	Base	Base asphalt	–
2	1%RHA-MA	Rice husk ash: Base asphalt	1:100
3	3%RHA-MA	Rice husk ash: Base asphalt	3:100
4	5%RHA-MA	Rice husk ash: Base asphalt	5:100
5	7%RHA-MA	Rice husk ash: Base asphalt	7:100
6	9%RHA-MA	Rice husk ash: Base asphalt	9:100
7	11%RHA-MA	Rice husk ash: Base asphalt	11:100
8	1%LA	Limestone filler: Base asphalt	1:100
9	5%LA	Limestone filler: Base asphalt	5:100
10	9%LA	Limestone filler: Base asphalt	9:100
11	15%BA	Bio-oil: Base asphalt	15:100
12	20%BA	Bio-oil: Base asphalt	20:100
13	30%BA	Bio-oil: Base asphalt	30:100
14	40%BA	Bio-oil: Base asphalt	40:100
15	RB-MA	Rice husk ash: Bio-oil: Base asphalt	1:20:100
16	5%RB-MA	Rice husk ash: Bio-oil: Base asphalt	5:20:100
17	9%RB-MA	Rice husk ash: Bio-oil: Base asphalt	9:20:100

analysis; the particle RI and dispersant RI was taken as 1.52 and 1.33, respectively. The chemical composites and density of bio-oil are presented in Table 2.

2.4. Physical property and rheological property test of asphalt binders

The physical properties of asphalt binders, including penetration, softening points and ductility, were tested according to ASTM D5 [27], ASTM D36 [28] and ASTM D 113–86 [29], respectively.

The Brookfield Viscometer was used to measure the apparent viscosity according to ASTM D4402 [30]. The DSR4000 dynamic shear rheometer was applied to characterize the rheological property of asphalt binders. Performance grade test and frequency scanning test from 0.1 rad/s to 100 rad/s with a fixed strain percentage of 10% at 40 °C, 50 °C, 60 °C and 70 °C were conducted according to ASTM D7175 [31] to obtain main curves of asphalt binders. Temperature creep test with angular frequency of 10 rad/s and strain percentage of 10% was conducted according to ASTM D7175[31] under temperature ranging from 45 °C to 70 °C with increment of 5 °C.

2.5. Scanning electronic microscopy test of asphalt binders

Hitachi S-4800 scanning electronic microscopy was utilized to observe the micro-structure of asphalt binders, while energy dispersive spectrometer was used to characterize the rice husk ash distribution by scanning of silicon element. For the observation with SEM, the asphalt samples were coated with gold in a sputter coater to obtain clearer SEM images. The SEM samples were observed at the acceleration voltage of 5 kV.

Finally, tests conducted in this work are summarized in flowchart shown in Fig. 3.

3. Modification effect of RHA

3.1. Physical properties of RHA-MA and LA

The physical properties of LA and RHA-MA are given in Fig. 4. It is obvious that RHA-MA possessed lower penetration values (at 15 °C, 25 °C, and 30 °C in Fig. 4a) and higher softening points (see

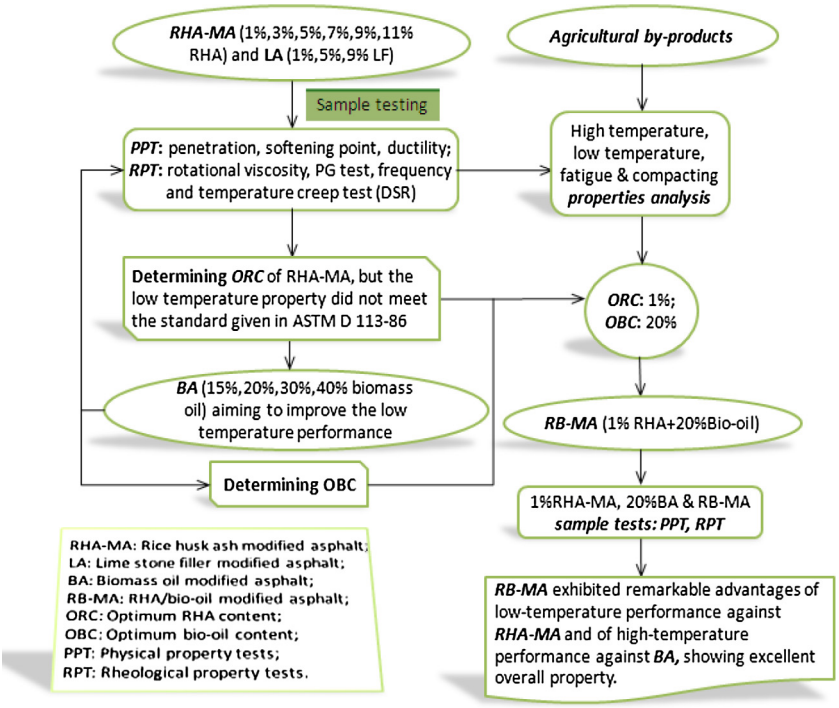

Fig. 3. Flow chart of laboratory tests.

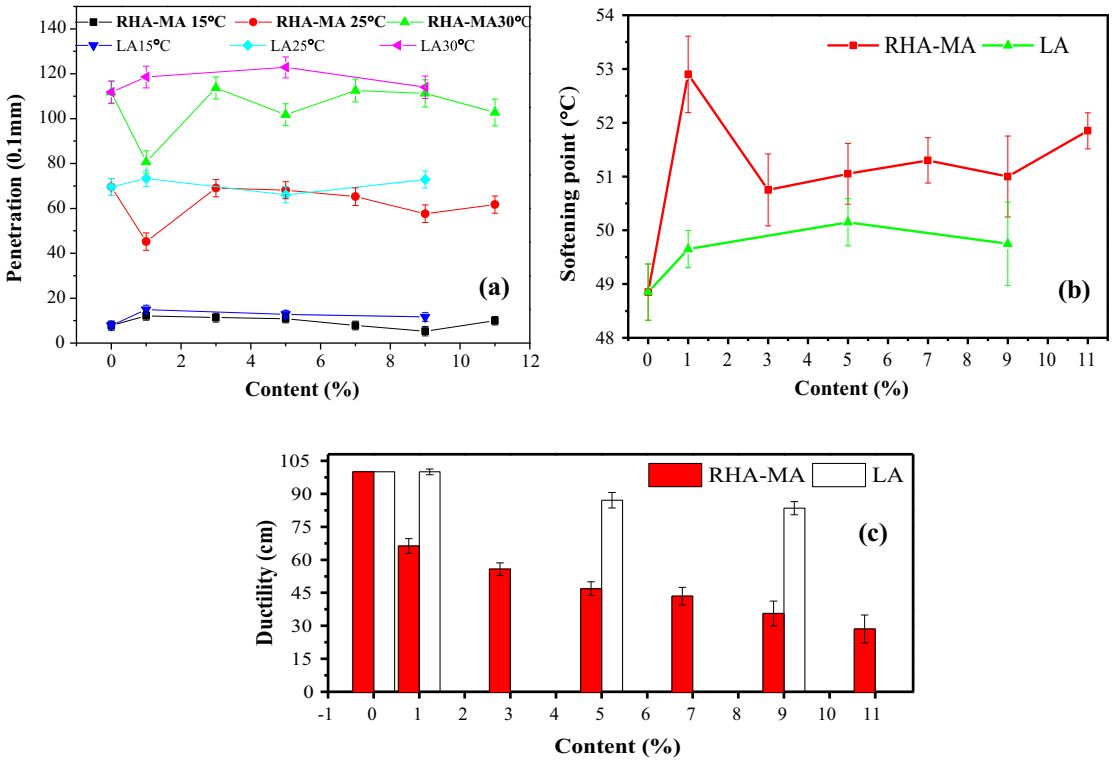

Fig. 4. Penetration (a), softening point (b) and ductility (c) comparison of RHA-MA, base asphalt and limestone filler mixed asphalt (LA).

Fig. 4b) than those of LA and base asphalt, indicating that RHA-MA possessed better high temperature properties. However, it can be observed from Fig. 4(c) that ductility of RHA-MA is remarkably less than that of LA, and the gap became greater as modifier contents increased, representing a deterioration trend of resistance against low temperature cracking.

Also, it can be observed that 1% RHA-MA obtained the highest softening point and ductility, the lowest penetration at 25 °C and 30 °C, and the highest penetration at 15 °C compared with other RHA contents, referring that 1% RHA seems to be the optimal choice for excellent overall performance of modified asphalt.

3.2. Rotational viscosity (RV) of RHA-MA and LA

RV test results at 60 °C and 135 °C are shown in Fig. 5. The viscosity of RHA-MA at 60 °C is higher than that of LA when the content is less than 4%, peaking at 400 Pa·s as RHA content was 1%. In marked contrast, LA sample was barely 186.7 Pa·s at the content of 1%. Thus, it seems that RHA-MA represents better high-temperature deformation resistance than LA at the typical high pavement service temperature.

RV test results at 135 °C suggest that viscosity of RHA-MA with RHA content less than 7% meet the upper limit of 3 Pa·s given in AASHTO T316 [32] considering the compatibility during pavement construction. Besides, 1% RHA-MA presented the lowest viscosity of 2.585 Pa·s at 135 °C, demonstrating the optimal compacting performance compared with other RHA-MA samples. Consequently, the optimal content and the upper RHA content limit obtained from RV test results was1% and 7%, respectively.

3.3. Dynamic Shear Rheometer (DSR) test of RHA-MA and LA

3.3.1. Performance grade test

Performance grade test results are presented in Fig. 6. It is evident that RHA-MA obtained failed temperature higher than LA on regard to all modifier contents, peaking at 72.9 °C. In marked contrast, fail temperature of 1% LA is 5.8 °C less than that of 1% RHA-MA.

The performance grade results of RHA-MA and LA samples are in line with that of fail temperature, demonstrating that RHA-MA samples possess better high-temperature property than LA. Also, 1% RHA content exhibits better modification effect for high temperature performance.

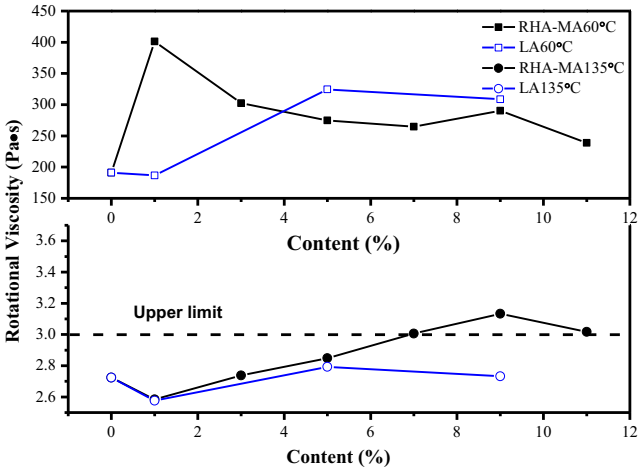

Fig. 5. Viscosity comparison of base asphalt, rice husk ash modified asphalt (RHA-MA) and limestone filler mixed asphalt (LA).

3.3.2. Dynamic frequency and temperature creep test

Frequency creep test results of RHA-MA and LA samples of all modifier contents presented identical tendency and pattern at different temperatures (40, 50, 60 and 70 °C). Thus, the temperature of 40 °C was selected as the representative condition for dynamic frequency creep test. Temperature creep test is adopted to comprehensively analyze the high temperature property of asphalt binders.

Complex shear modulus (G^*) and phase angle (δ) are the basic parameters of DSR test. G^* is the characterization of resistance to deformation when asphalt binder is repeatedly sheared (Eq. (1)). Phase angle is a measurement of the elastic and plastic proportion of asphalt binder. These two parameters are usually utilized to evaluate the rutting and fatigue performance of asphalt binder by calculating $G^*/\sin\delta$ and $G^* \times \sin\delta$, respectively.

$$G^* = \frac{\tau_{max}}{\gamma_{max}} \tag{1}$$

In which

$$\tau_{max} = \frac{2T}{\pi r^3} \tag{2}$$

$$\gamma_{max} = \frac{\theta}{h} * r \tag{3}$$

where: τ_{max}: Maximum applied stress; γ_{max}: Maximum resultant strain; T:Maximum applied torque; r: Specimen radius; θ: Deflection angle; h: Specimen height.

Fig. 7(a and b) show that 1%RHA-MA obtained the highest complex modulus compared with other RHA contents (see Fig. 7a) and all LA samples, as well as base asphalt (see Fig. 7b). Furthermore, it can be observed from G^* main curves of base asphalt, 1% RHA-MA and 1% LA in Fig. 7(c) that 1% RHA-MA presents the highest G^* on the whole range of angular frequency from 1×10^{-4} rad/s to

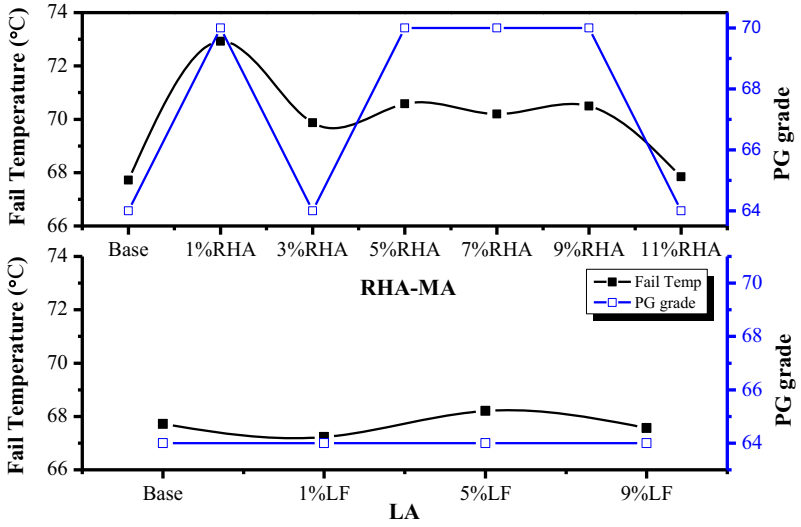

Fig. 6. Performance grade and fail temperature of base asphalt, rice husk ash modified (RHA-MA) and limestone filler mixed asphalt (LA) samples.

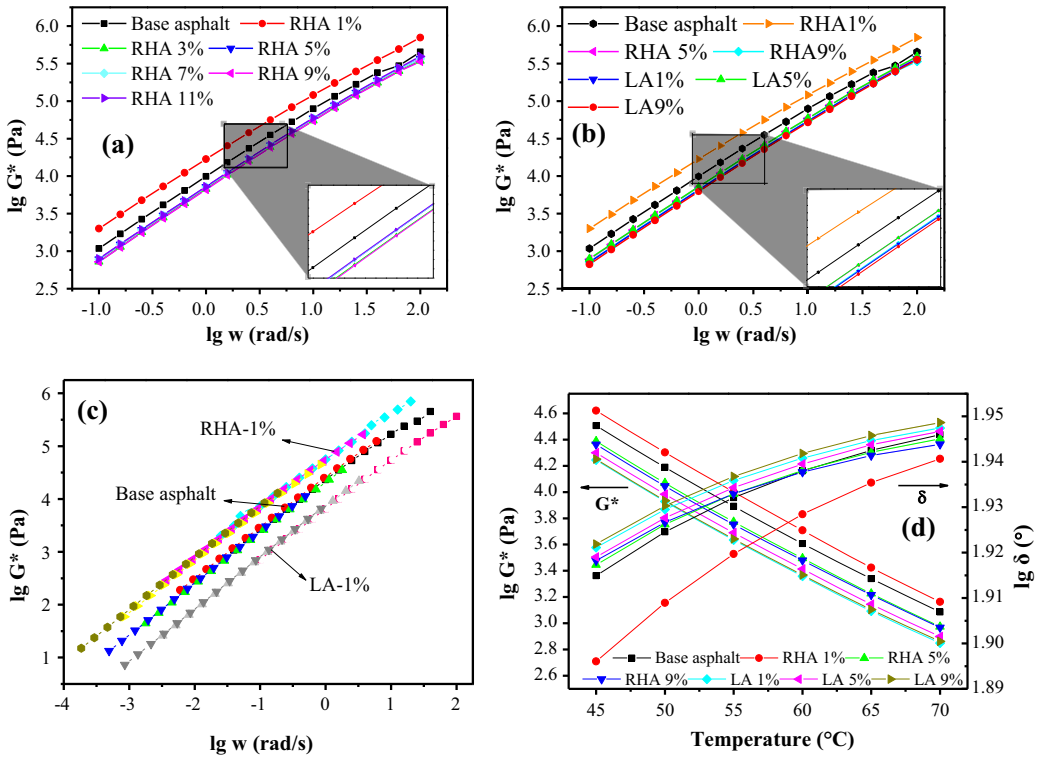

Fig. 7. Complex modulus of base asphalt and rice husk ash modified asphalt samples (a), of base asphalt, limestone filler mixed asphalt and rice husk ash modified asphalt (b); main curves of base asphalt, rice husk ash modified asphalt and limestone filler mixed asphalt with modifier content of 1% at 40 °C (c); complex modulus and phase angle of base asphalt, rice husk ash modified asphalt and limestone filler asphalt mortar at different temperature (d).

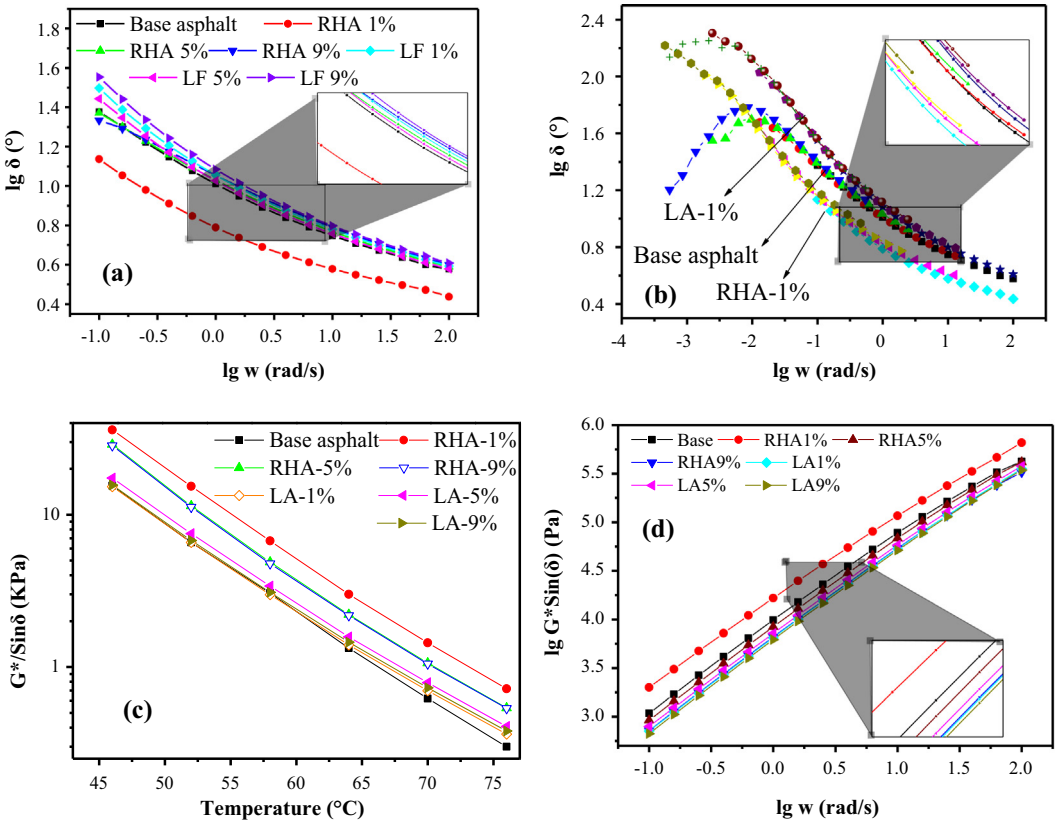

Fig. 8. Phase angle comparison of base asphalt, rice husk ash modified asphalt and limestone filler mixed asphalt (a), Phase angle main curves of base asphalt, rice husk ash modified and limestone filler mixed asphalt at 40 °C (b), rutting factor comparison of base asphalt, rice husk ash modified asphalt and limestone filler mixed asphalt with corresponding modifier contents at different temperatures (c), and loss modulus comparison of base asphalt, rice husk ash modified asphalt and limestone filler mixed asphalt at 40 °C (d).

100 rad/s. Besides, temperature creep test results shown in Fig. 7 (d) demonstrated that 1%RHA-MA possessed the highest G* and the lowest phase angle within the whole temperature range (45–70 °C), indicating better high temperature and plastic deformation resistance performance than base asphalt and LA.

Phase angle results of RHA-MA, LA and base asphalt are presented in Fig. 8 (a) and (b). It is evident that 1% RHA-MA obtained the lowest phase angle among all samples, indicating the best plastic deformation resistance. Besides, phase angle results of other RHA-MA and LA samples fluctuated around that of base asphalt (see Fig. 8a), showing no obvious improvement for the elastic deformation recovery property.

Phase angle (δ) main curves of base asphalt, 1% RHA-MA and 1% LA expands the angular frequency (w) range from 0.1 rad/s–100 rad/s to 0.0001 rad/s–100 rad/s according to test results at 40, 50, 60, 70 °C based on time–temperature equivalence principle (see Fig. 8b). As characterization of loading rate, the expanded angular frequency range is able to reveal more complete rheological properties of asphalt binder under a wider scale of loading rate. As is illustrated in Fig. 8b, δ of RHA-1% is apparently less than and generally show similar downward trend as that of LA and base asphalt. Noticeably, the irregular δ peak of base asphalt appeared at w of 0.01 rad/s was attributed to the fact that the part of data was collected at temperature (70 °C) higher than its fail temperature 67.2 °C. Therefore, δ measured at 70 °C under low angular frequency less than 0.01 rad/s is invalid, and 1% RHA-MA seems to obtain the best plastic deformation resistance property.

Fig. 8(c) shows the rutting factor (G*/Sinδ) of base asphalt, RHA-MA and LA. It can be observed that 1% RHA-MA possessed the highest G*/Sinδ at all temperatures, followed by 5 and 9%RHA-MA, leaving LA and base asphalt with similar lower rutting factor values. Hence, it is likely that RHA-MA has better permanent deformation resistance than LA and base asphalt at the typical asphalt pavement service temperature ranging from 40 °C to 70 °C, and 1% RHA presented better modification effect compared with other RHA contents and LF. The loss modulus of base asphalt, RHA-MA and LA indirectly representing the anti-fatigue performance of asphalt binder are presented in Fig. 8(d). It can be seen that LA and 9%RHA-MA showed similar loss modulus which was less than that of base asphalt, indicating better anti-fatigue performance than base asphalt. It can be referred from the loss modulus test result that the addition of inorganic ash enhanced the cohesive strength of asphalt binder and reduce the energy loss when asphalt experienced repeated deformation, making asphalt binder more reliable against fatigue damage. However, 1%RHA-MA presented higher G*×Sinδ than base asphalt, and 5%RHA-MA illustrated similar value to base asphalt, which might have been attributed to the reason that the insufficient asphalt cohesion formed by RHA and base asphalt when the content was less than 5%, as well as the stress concentration caused by the irregular-shaped RHA blocks.

Therefore, it can be concluded that RHA-MA obtained better comprehensive mechanical, elastic deformation recovery and permanent deformation resistance performance than base asphalt and LA. 1% RHA could be the optimal choice for excellent high temperature and comprehensive mechanical performance, although it demonstrated undesirable low temperature and anti-fatigue properties. In order to make use of the excellent high temperature performance of RHA-MA to produce modified asphalt with desirable comprehensive performance, 1%RHA-MA was selected to conduct further modification utilizing the viscosity reducer bio-oil.

4. Modification of RHA-MA with bio-oil

Physical and rheological tests of RHA-MA, LA and base asphalt have proven that 1% RHA could effectively improve the high-temperature property of asphalt binder. The low-temperature property (ductility, 15 °C), however, decreased sharply from 120 cm (base asphalt) to 66.3 cm (1% RHA-MA), and was about 40 cm less than that of 1% LA. Besides, 1%RHA-MA presented unfavorable loss modulus value compared with base asphalt and LA. Thus, the viscosity reducing modifier, bio-oil, was utilized to cooperate with RHA to improve the low-temperature and anti-fatigue properties of RHA-MA.

4.1. Physical property of BA, RHA-MA and RB-MA

The physical properties of BA are presented in Fig. 9. In general, penetration at 25 °C and ductility at 10 °C increased steadily as the bio-oil content keep growing, while softening point experienced a gradual decline instead. Thus, bio-oil is able to reduce the viscosity of asphalt binder, enhancing the low-temperature properties and weakening high-temperature performance. However, 20% BA presented desirable high temperature and relatively excellent low temperature properties compared with other contents. Consequently,

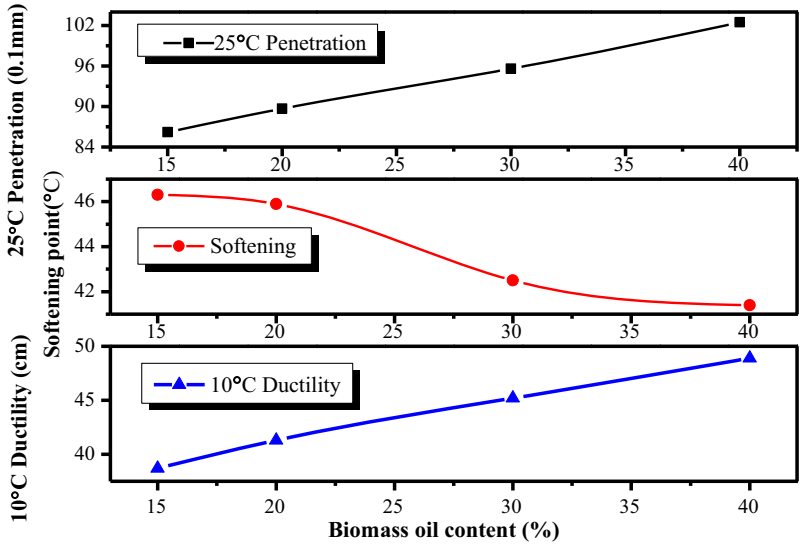

Fig. 9. Physical properties of bio-oil modified asphalt.

together with 1% RHA, this study selected 20% bio-oil to prepare modified asphalt with excellent comprehensive performance.

Physical properties comparison among RHA-MA, BA, RB-MA and base asphalt samples are demonstrated in Fig. 10(a) and (b). BA sample presented the highest penetration, ductility and the lowest softening point, indicating that BA obtained the best low temperature property but the poorest high temperature performance among all asphalt samples. In contrast, the penetration and softening point of RB-MA is almost 20 (0.1 mm) lower and 4 °C higher than that of BA, demonstrating the effective improvement of high temperature property brought by RHA. Besides, the ductility of RB-MA exceeds about 30 cm, almost half of RHA-MA, indicating that bio-oil remarkably improves the low temperature anti-cracking property of RHA-MA.

4.2. Rheological property of BA, RHA-MA and RB-MA

Dynamic frequency and temperature creep results are shown in Fig. 11. As is shown in Fig. 11(a), G* of RB-MA is higher than that of BA, indicating that RHA enhanced the comprehensive mechanical property of BA; while RHA did not make obvious improvement on the phase angle of RB-MA compared with BA, and RB-MA obtained no better plastic deformation resistance than base asphalt and RHA-MA. Accordingly, modification of BA by RHA could only slightly enhance its mechanical property and provide little help with the plastic deformation resistance. Besides, temperature creep test results shown in Fig. 11(b) were in line with that of frequency test, illustrating that RHA could improve the mechanical performance but offered little help to the plastic deformation resis-

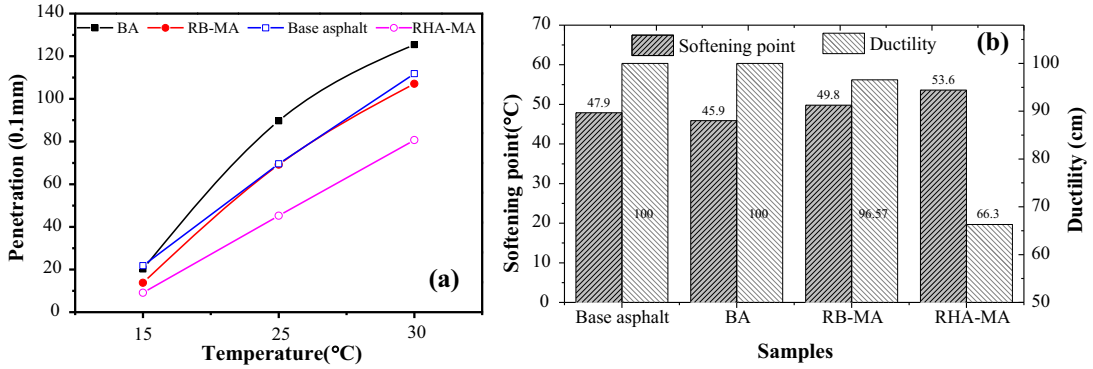

Fig. 10. Penetration comparison (a), softening point and ductility comparison (b) of different asphalt samples.

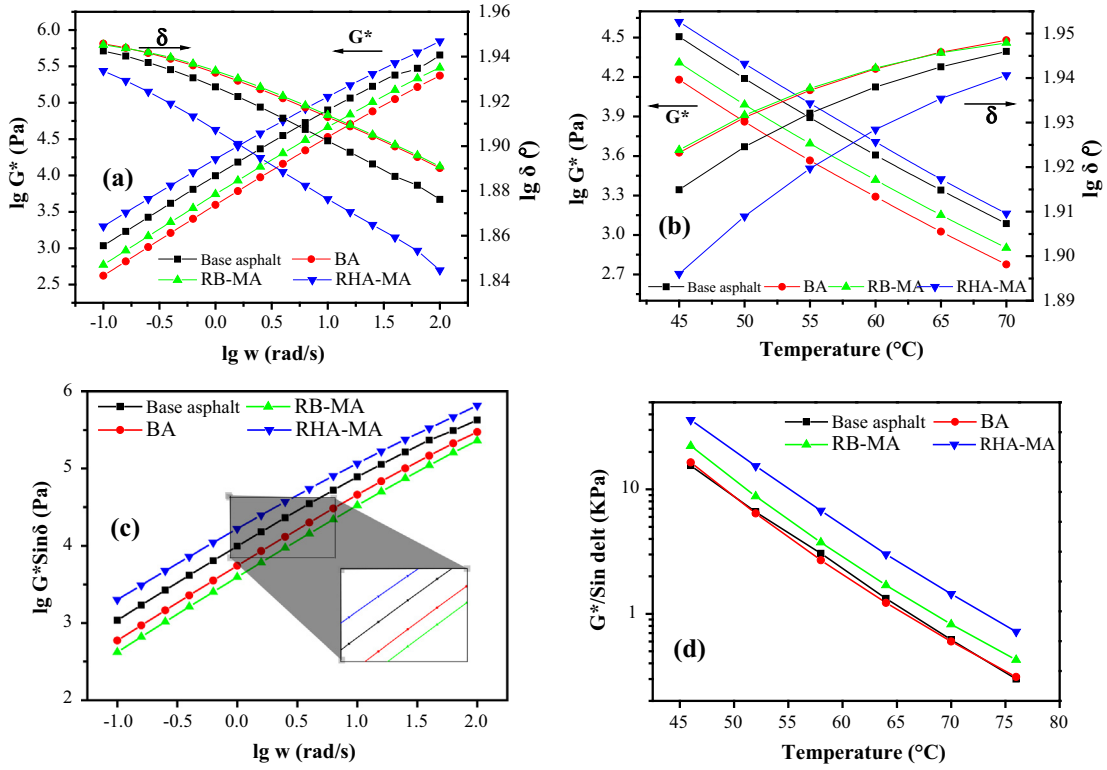

Fig. 11. Complex modulus and phase angle of base asphalt, rice husk ash modified asphalt, bio-oil modified asphalt and rice husk ash/bio-oil modified asphalt at different frequency (a), at different temperature (b); loss modulus (c) and rutting factor (d) comparison of the base asphalt, bio-oil modified asphalt, rice husk ash/bio-oil modified asphalt and rice husk ash modified asphalt.

tance of BA under temperature ranging from 45 to 70 °C. However, it is the aggregate in asphalt mixture that is mainly responsible for mechanical supporting and deformation resisting. Therefore, it is acceptable that RB-MA is not as well-behaved at mechanical performance as RHA-MA.

The loss modulus reflects the energy loss in form of heat when asphalt binder experiences deformation, indirectly characterizing the anti-fatigue capability of asphalt binder. As can be seen in Fig. 11 (c), RB-MA possessed the lowest loss modulus, even slightly less than that of BA, while RHA-MA presented the highest loss modulus instead. Consequently, it is likely that RB-MA obtained excellent anti-fatigue performance even better than that of BA owing to the cooperated modification of RHA and bio-oil, while RHA-MA possessed the most undesirable fatigue damage resistance. The improvement of anti-fatigue performance for RHA modified asphalt could have been achieved by the viscosity reducing and RHA/asphalt interface enhancing effect of bio-oil.

$G^*/\sin\delta$ results shown in Fig. 11(d) illustrate that RHA-MA presented the highest rutting factor under temperature ranging from 46 to 76 °C, followed by RB-MA. Not surprisingly, RHA-MA presented the best high-temperature deformation resistance, but it can also be summarized that RB-MA obtain much better

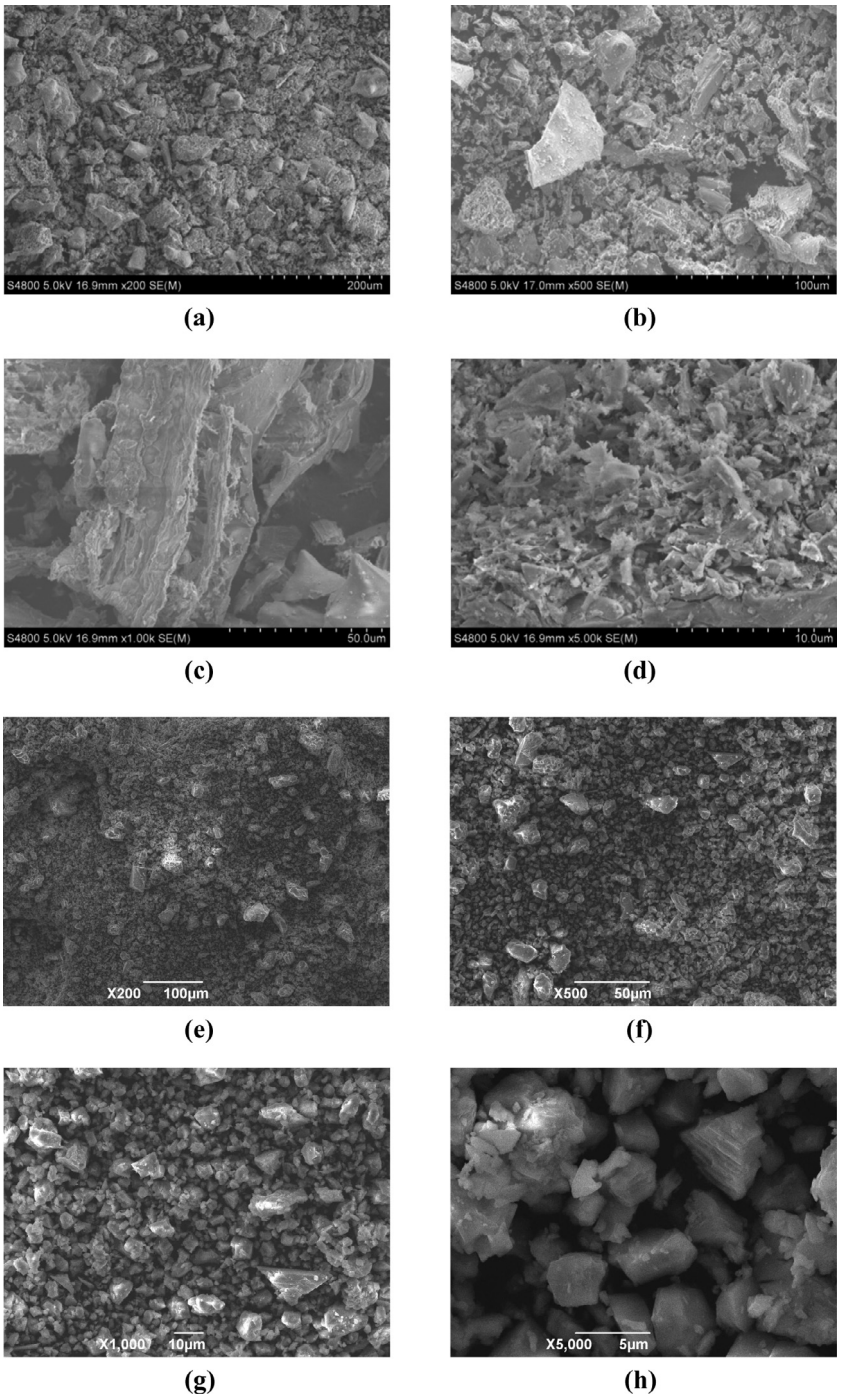

Fig. 12. SEM images of rice husk ash at magnifications of ×200 (a), ×500 (b), ×1000 (c) and ×5000 (d); of limestone filler at magnification of ×200 (e), ×500 (f), ×1000 (g) and ×5000 (h).

permanent deformation resistance and high temperature stability at typical high asphalt pavement service temperature (40–70 °C) than BA and base asphalt.

Finally, it seems from physical and rheological test results that the modification of RHA-MA by bio-oil greatly enhanced the low-temperature and anti-fatigue properties, in spite of a small degree decline of mechanical performance that can be compensated by the supporting of aggregate in asphalt mixture. In conclusion, RHA/bio-oil could be a promising asphalt modifier to combine desirable high-temperature performance of RHA-MA, excellent low-temperature and anti-fatigue performance of BA, making RB-MA obtain desirable comprehensive performance qualified for the demand of complex pavement service ambient conditions.

5. Modification mechanism of RHA and bio-oil

5.1. Modification mechanism of RHA

Scanning electron micrographs observed at magnifying power of ×200 and ×500 are shown in Fig. 12(a and b). Irregular flakes and blocks with sizes (maximum length or width) ranging from several microns to about 600μm can be seen in the microstructure

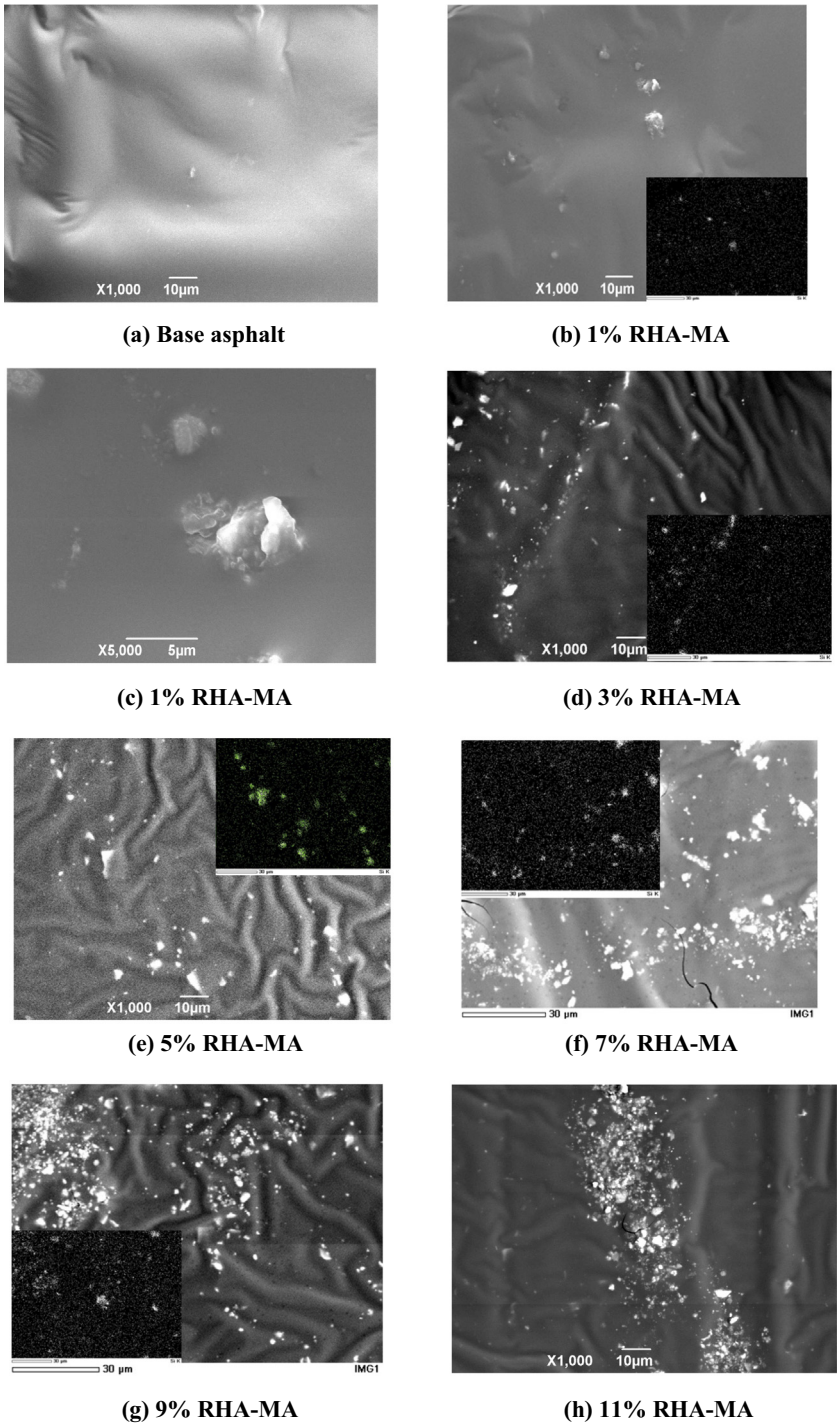

(a) Base asphalt (b) 1% RHA-MA

(c) 1% RHA-MA (d) 3% RHA-MA

(e) 5% RHA-MA (f) 7% RHA-MA

(g) 9% RHA-MA (h) 11% RHA-MA

Fig. 13. Scanning electron micrographs and energy dispersive X-ray spectrometer analysis of rice husk ash modified asphalt and base asphalt.

of RHA. In marked contrast to the spherical modifier particles, the irregular-shaped blocks are very likely to generate sever stress concentration in asphalt binder, making the modified asphalt more prone to fail in low-temperature test (such as ductility). However, the microstructure of RHA is a three-dimensional porous and multi-layer system: the exterior layer, interior layer and interlayer, as can be observed in the cross section SEM image of RHA in Fig. 12 (c). Xu et al. [3] have obtained similar results and drawn the conclusion that the interlayer is consisted of a crisscross mesh of chips and pores ranging from several nanometers to several microns. The multilayer structure and micro-pores in RHA contributed greatly to the adhesive property of modified asphalt.

It can be seen from Fig. 12(c) that the surface of the exterior layer and interior layer was rough. Further magnified SEM image of the exterior layer surface presented in Fig. 12 (d) indicates that the surface of micro RHA particle was consisted of microchips and micro sheets in three-dimensional reticular distribution. Moreover, white columnar SiO_2 crystal whiskers found on the surface and edges of the microchips and micro sheets might generate attraction between SiO_2 crystal whiskers and base asphalt. In remarkable comparison, the shape and size of limestone filler particles were found to be more regular and uniform than that of RHA in the SEM images of LF in Fig. 12(e and f). Different from the three-dimensional porous and multi-layer system of RHA, limestone filler particles presented as dense solid particles in Fig. 12(g) which can be further validated in Fig. 12(h). As a result, the adhesion between LF and base asphalt was weaker and the stress concentration degree was less than that between RHA and base asphalt. Besides, it can be observed from Fig. 12(h) that the surface of limestone filler particles was commonly smooth and appeared no white columnar crystal whiskers as RHA did. Consequently, RHA could form a more stable and viscous three-dimensional meshed bonding system with base asphalt than limestone filler or other mineral asphalt modifiers, effectively increasing the high temperature plastic deformation resistance performance and adhesion property.

5.2. Modification mechanism of bio-oil

The SEM and EDS images of base asphalt, RHA-MA and RB-MA with different RHA contents are demonstrated in Figs. 13 and 14. The EDS images of silicon verified that the light particles observed in SEM images are RHA particles.

As is shown in Fig. 13, agglomeration was more prone to occur as RHA content increased from 1% to 11%, referring the inhomogeneous mix of RHA and base asphalt. In marked contrast to RHA-MA samples, the addition of bio-oil into RHA-MA with 1, 5 and 9% RHA can obviously improve the mixing uniformity of RHA-MA binder, which can be observed in Fig. 14. Therefore, it is likely that the increase of penetration, the decrease of softening point and sharply drop of RHA-MA ductility as RHA content increased might have been caused by the agglomeration of RHA. And mixing uniformity enhancement of RB-MA binder derived from the addition of bio-oil make great contribution to the improved low temperature anti-cracking (ductility) and anti-fatigue performance (see Fig. 11c).

Furthermore, the ideal bonding system (see the schematic diagram in Fig. 15) formed by RHA, bio-oil and base asphalt can be obtained according to SEM analysis of RHA and RB-MA. As is illustrated in Fig. 15, the addition of bio-oil is conducive to the uniform dispersion of RHA and sufficiently filling of asphalt in the voids and micro-structure of RHA particles, providing a more stable adhesive system and stronger bonding function in the interface of asphalt binder and irregular RHA particles. These modification effects of bio-oil can be validated by the aforementioned comparative SEM and EDS analysis of RHA-MA and RB-MA samples. Consequently, rice husk ash and base asphalt could be bonded more closely by the three-dimensional crisscross meshed adhesive system, enabling the RB-MA acquire desirable high-temperature, low-temperature and anti-fatigue performance.

However, it can be seen in Fig. 14 that the increasing amount of RHA in RB-MA would also cause agglomeration. Apparently, RB-MA with 1% RHA and 20% bio-oil demonstrated the most uni-

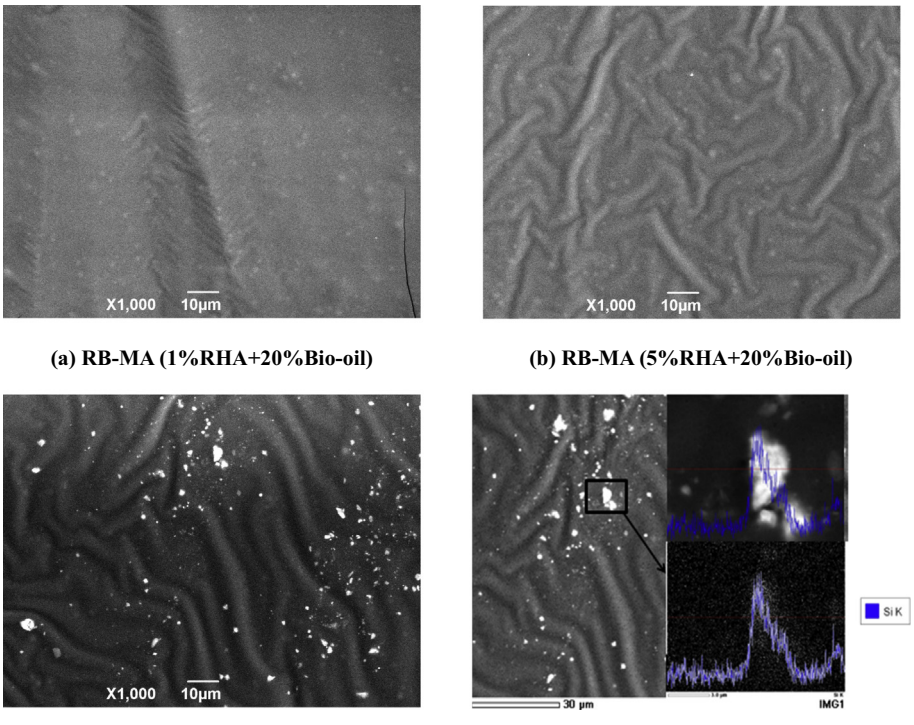

(a) RB-MA (1%RHA+20%Bio-oil) **(b) RB-MA (5%RHA+20%Bio-oil)**

(c) RB-MA (9%RHA+20%Bio-oil) **(d) Partially enlarged view of (c)**

Fig. 14. Scanning electron micrographs and energy dispersive X-ray spectrometer analysis of rice husk ash/ bio-oil modified asphalt.

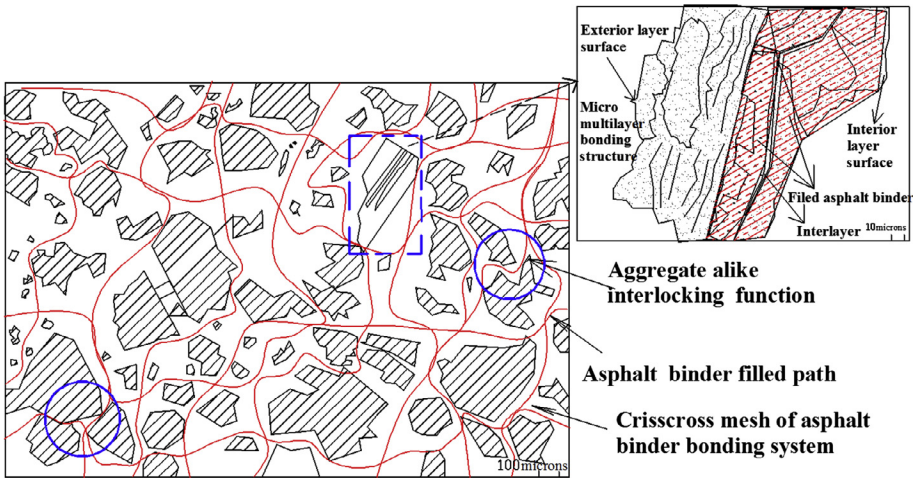

Fig. 15. Schematic diagram of the bonding system formed by rice husk ash and base asphalt.

form modifier distribution. This is also in good agreement with the test results that the modification of RHA-MA by bio-oil significantly improved the ductility and reduce the loss modulus, while the high-temperature properties such as penetration (at 30 °C), complex modulus and rutting factor of RB-MA did not experience obvious reduction.

Therefore, it can be concluded that bio-oil can effectively improve the low-temperature and anti-fatigue performance of RHA-MA by providing a uniformly mixed modified asphalt system. 1% RHA and 20% bio-oil is the optimal content for RB-MA to achieve the desirable balance between high-temperature and low-temperature properties.

6. Conclusion

In this study, agricultural by-product RHA (1–11%) was utilized as modifier to prepare modified asphalt. Physical and rheological property test results indicated that the addition of RHA can dramatically improve the high-temperature performance of base asphalt. 1% RHA was confirmed to be the optimum content for 70# base asphalt modification and 7% was determined as the upper content limit for compatibility demand during pavement construction. However, RHA-MA samples presented unsatisfactory low-temperature and anti-fatigue performance, greatly limiting its application in the pavement.

Bio-oil was utilized to ameliorate the viscosity increasing effect of RHA. Test results prove that the modification of RHA-MA with bio-oil can effectively improve the low temperature and anti-fatigue performance, as well as maintain qualified high temperature performance, making RHA/bio-oil the optimal modifier combination to achieve the balance between high temperature and low temperature performance.

SEM and EDS analysis are adopted to explore the modification mechanism of RHA and bio-oil. Results indicate that the crisscross mesh of irregular chips and micro pore structure of RHA could be the main reasons why RHA-MA obtained excellent high-temperature performance. The ideal bonding system and uniformity of RB-MA obtained by the addition of bio-oil contributed the most to the excellent overall performance of RB-MA.

Acknowledgements

This study was finally supported by the Construction Technology Project of Ministry of Transport of China (Grant No. 2013318221150) and the Natural Science Basic Research Plan in Shaanxi Province of China (Grant No. 2015KJXX-23).

Additionally, authors are also grateful for the remarkable attribution made by Prof. Liqun Hu, Prof. Feng Ma and Prof. Wei Jiang in equipment providing and paper revising.

References

[1] USDA ERS - Rice: Trade. http://www.ers.usda.gov/topics/crops/rice/trade (accessed August 5, 2016).
[2] Nick Zemke, Emmet Woods, Rice Husk Ash, California Polytechnic State University, 2009.
[3] W. Xu, T.Y. Lo, S.A. Memon, Microstructure and reactivity of rich husk ash, Constr. Build. Mater. 29 (2012) 541–547.
[4] D.P. Kumar, A.K. Anupam, Waste Materials-An Alternative to Conventional Materials in Rural Road Construction, in: Workshop Non-Conv. Mater. Cent. Road Res. Inst. New Delhi, 2012: pp. 16–26.
[5] M. Alhassan, Potentials of rice husk ash for soil stabilization, Assumpt. Univ. J. Technol. 11 (2008) 246–250.
[6] A.S. Muntohar, Utilization of uncontrolled burnt rice husk ash in soil improvement, Civ. Eng. Dimens. 4 (2004) 100.
[7] K.M. Anwar, Hossain, stabilized soils incorporating combinations of rice husk ash and cement kiln dust, J. Mater. Civ. Eng. 23 (2011) 1320–1327.
[8] M. Nehdi, J. Duquette, A. El Damatty, Performance of rice husk ash produced using a new technology as a mineral admixture in concrete, Cem. Concr. Res. 33 (2003) 1203–1210.
[9] J. Wei, C. Meyer, Utilization of rice husk ash in green natural fiber-reinforced cement composites: mitigating degradation of sisal fiber, Cem. Concr. Res. 81 (2016) 94–111.
[10] P.K. Mehta, Properties of blended cements made from rice husk ash, ACI J. Proc., 74, ACI, 1977, pp. 440–442.
[11] M.-H. Zhang, V.M. Malhotra, High-performance concrete incorporating rice husk ash as a supplementary cementing material, ACI Mater. J. 93 (1996) 629–636.
[12] D.D. Bui, J. Hu, P. Stroeven, Particle size effect on the strength of rice husk ash blended gap-graded Portland cement concrete, Cem. Concr. Compos. 27 (2005) 357–366.
[13] M.S. Ismail, A.M. Waliuddin, Effect of rice husk ash on high strength concrete, Constr. Build. Mater. 10 (1996) 521–526.
[14] Y.E. Guang, V.T. Nguyen, Mitigation of autogenous shrinkage of ultra-high performance concrete by rice husk ash, J. Chin. Ceram. Soc. 40 (2012) 212–216.
[15] Ha Thanh Le, Horst-Michael Ludwig, Effect of rice husk ash and other mineral admixtures on properties of self-compacting high performance concrete, Mater. Des. 85 (2016) 156–166.
[16] P. Chindaprasirt, S. Rukzon, Strength, porosity and corrosion resistance of ternary blend Portland cement, rice husk ash and fly ash mortar, Constr. Build. Mater. 22 (2008) 1601–1606.
[17] M.C. Nataraja, Y. Nalanda, Performance of industrial by-products in controlled low-strength materials (CLSM), Waste Manag. 28 (2008) 1168–1181.
[18] K. Ganesan, K. Rajagopal, K. Thangavel, Rice husk ash blended cement: assessment of optimal level of replacement for strength and permeability properties of concrete, Constr. Build. Mater. 22 (2008) 1675–1683.
[19] Şebnem Sargın, M. Saltan, N. Morova, S. Serin, S. Terzi, Evaluation of rice husk ash as filler in hot mix asphalt concrete, Constr. Build. Mater. 48 (2013) 390–397.
[20] X. Guo, M. Sun, W. Dai, S. Chen, Performance characteristics of silane silica modified asphalt, Adv. Mater. Sci. Eng. 2016 (2016).
[21] Y. Xue, S. Wu, J. Cai, M. Zhou, J. Zha, Effects of two biomass ashes on asphalt binder: dynamic shear rheological characteristic analysis, Constr. Build. Mater. 56 (2014) 7–15.

[22] X. Yang, Z. You, Q. Dai, J. Mills-Beale, Mechanical performance of asphalt mixtures modified by bio-oils derived from waste wood resources, Constr. Build. Mater. 51 (2014) 424–431.
[23] E.H. Fini, S.-H. Yang, S. Xiu, Characterization and application of manure-based bio-binder in asphalt industry, in: Transp. Res. Board 89th Annu. Meet., 2010. http://trid.trb.org/view.aspx?id=910772. (accessed March 4, 2016).
[24] Z. You, J. Mills-Beale, E. Fini, S.W. Goh, B. Colbert, Evaluation of low-temperature binder properties of warm-mix asphalt, extracted and recovered RAP and RAS, and Bioasphalt, J. Mater. Civ. Eng. 23 (2011) 1569–1574.
[25] E. Fini, D. Oldham, F.S. Buabeng, S.H. Nezhad, Investigating the Aging Susceptibility of Bio-modified Asphalts, Airfield Highw. Pavements Conf., The American Society of Civil Engineers, Miami, FL, 2015.
[26] RIOH, Technical Specification for Construction of Highway Asphalt Pavements (JTG F40-2004), China Communications Press, Beijing, 2004 [in Chinese].
[27] ASTM D5, Standard Test Method for Penetration of Bituminous Materials, Annual Book of ASTM Standards USA, 1992.
[28] ASTM D36, Standard Test Method for Softening Point of Bitumen (Ring-and-ball Apparatus), Annual Book of ASTM Standards USA, 1992.
[29] ASTM D113, Standard test method for ductility of bituminous materials, Annual Book of ASTM Standards USA, 1992.
[30] ASTM D4402, Standard test method for viscosity determination of asphalt, Annual Book of ASTM Standards USA, 2006.
[31] ASTM D7175, Standard test method for determining the rheological properties of asphalt binder using a dynamic shear rheometer, Annual Book of ASTM Standards USA, 2007.
[32] AASHTO, AASHTO T 316: Standard Method of Test for Viscosity Determination of Asphalt Binder Using Rotational Viscometer, American Association of State Highway and Transportation Officials, 2006.